A comprehensive theoretical approach for analysing manoeuvring effects on ships by integrating hydrodynamics and power system

Nasiri, Saman; Peyghami, Saeed; Parniani, Mostafa; Blaabjerg, Frede

Published in:
I E T Electrical Systems in Transportation

DOI (link to publication from Publisher):
10.1049/els2.12040

Publication date:
2022

Document Version
Publisher's PDF, also known as Version of record

Citation for published version (APA):
Nasiri, S., Peyghami, S., Parniani, M., & Blaabjerg, F. (2022). A comprehensive theoretical approach for analysing manoeuvring effects on ships by integrating hydrodynamics and power system. *I E T Electrical Systems in Transportation*, *12*(2), 89-101. https://doi.org/10.1049/els2.12040

Received: 27 November 2020 | Revised: 12 October 2021 | Accepted: 26 October 2021

DOI: 10.1049/els2.12040

IET Electrical Systems in Transportation

The Institution of Engineering and Technology WILEY

ORIGINAL RESEARCH PAPER

A comprehensive theoretical approach for analysing manoeuvring effects on ships by integrating hydrodynamics and power system

Saman Nasiri[1] | Saeed Peyghami[2] | Mostafa Parniani[1] | Frede Blaabjerg[2]

[1]Department of Electrical Engineering, Sharif University of Technology, Tehran, Iran

[2]Department of Energy Technology, Aalborg University, Aalborg, Denmark

Correspondence

Saman Nasiri, Department of Electrical Engineering, Sharif University of Technology, Tehran, Iran.
Email: Saman.nasiri@ee.sharif.edu

Abstract

Ship motions affect the propulsion system, which causes fluctuations in the power system. Mutually, the power system variations impact the ship velocity by generating speed changes in the propeller. Therefore, interconnecting the ship hydrodynamic and power system has paramount importance in designing and analysing an all-electric ship (AES). The lack of an integrated model that can be evaluated in various operating conditions, such as manoeuvring, is evident. This paper explores the required perceptions for the power system and hydrodynamic analysis of an AES. Then, an integrated theoretical model comprising both the ship motion and power system is proposed. In addition to providing an accurate model for the ship in varying situations, this study demonstrates that the ship speed estimation during a ship route change differs from when the interconnections are overlooked. In the light of this determination, a straightforward enhancement for the ship speed control system is proposed. The effects of this modification on the ship power system are explored using the proposed model. The developed model is examined in different scenarios, and its advantages are discussed. It is shown that this model is suitable for employing in the model-based design of AESs.

KEYWORDS

marine power systems, marine propulsion, ships

1 | INTRODUCTION

After introducing the electrical propulsion system and its benefits, naval organizations have widely welcomed the all-electric ship (AES) concept during the last decade. Formerly, the electric power level in ships was a few megawatts and mainly was used for typical electric power loads like ship services. With the advent of the electric propulsion system, the electric power level has been significantly raised in AES [1]. The integrated power system used in AES makes it easier to control all aspects of the power system. This capability can lead to increased reliability, power quality, and efficiency of the power system performance [2]. Utilizing electric propellers resulted in more advanced energy management and decreasing fuel and greenhouse gas emission. On the other hand, this interconnection generated critical control and operation challenges [3]. Since the naval propulsion system has a unique dynamics and is impacted by the ship motion, these challenges necessitate novel solutions that were not essential for typical terrestrial microgrids.

The electrical load of a propulsion system fluctuates due to various impacts from waves or in-and-out-water effects [4]. Several studies aimed to explore the impact of these variations on the ship power system. Some of these fluctuations exist particularly in a marine power system. A control method focussing on energy storage control is presented in Ref. [5], and power fluctuations and the cost of energy storage systems are reduced by optimizing the configuration of the battery and supercapacitor. Likewise, analytic equations for the estimation of system marginal cost of a ship power system equipped with energy storage and photovoltaic system are obtained in Ref. [6], and the economic operation of this system is analysed. A model predictive control system for mitigation of harmonics in a diesel-electric ship is discussed in Ref. [7]. Here, the authors studied a microgrid with two harmonic load buses and recommended a method to mitigate the harmonics in the microgrid by taking advantage of an active power filter. In Ref. [8], a load re-distribution controller for compensating frequency fluctuations of a ship power system is provided. In addition, one of the power quality problems in a ship electric network is voltage and frequency modulation. In Refs. [9, 10], in a series of two companion papers, the theoretical analysis of voltage and frequency modulation is established by highlighting the critical parameters affecting them. Then, the modulations are expressed, comprising several parameters of an AES power system.

A few studies are focussed on the dynamic stability of an AES power system and different approaches are analysed for properly controlling and stabilizing the power system. In Ref. [11], dynamic and mathematical modelling for stability analysis of onboard DC power systems is presented. It emphasized the power electronic parts of the power system. In Ref. [12], a model for different components of an AES power system is presented. It provided a model for uncontrolled full-bridge rectifiers and suggested a model predictive algorithm for stabilizing the DC voltage. A control strategy that improves the stability of MVDC bus voltage in the presence of destabilizing constant power load converters is presented in Ref. [13]. This adaptive control is capable of solving the problem of voltage instability induced by incremental negative resistance of constant power load converters. Ref. [14] examines alternative models of propulsion system components, with an emphasis on propeller drive models. In Ref. [15], simulations are performed for various frequencies of load fluctuations in a ship power system, and the results are evaluated. A power management strategy for mitigating the torque fluctuations and enhancing the propeller lifespan is presented in Ref. [16]. A simulator for maritime vessels is presented in Ref. [17] by considering the navigation and power systems. Ref. [18] discussed AES modelling with DC hybrid power systems. Although these models subtly depict load variations in the power system in dynamic positioning conditions, the impact of ship movements on the power system in a manoeuver and change of route operation is overlooked. Furthermore, the primary focus of the previously stated studies is either the AES power system or the ship motion in a specific operating condition. Thus, the lack of a model that considers both these concepts in different situations is evident.

The above-mentioned investigations have found some attractive solutions for the challenges in AES power systems. However, they have commonly used system models in their studies with a notable lack of precision. Common issues in the previous works are: (1) The propulsion system dynamics are not modelled thoroughly. In some studies, only a constant load profile or torque pattern has been used. Neglecting the particular characteristics of the propeller load in different operational conditions can result in uncertain dynamics and instability of the ship. (2) The power system and propulsion system interconnections are not investigated precisely. Power system fluctuations caused by the ship's typical loads can impact the propulsion system functionality. Disregarding these impacts can affect ship speed and position estimations in the ship control system. On the other hand, propulsion torque fluctuations caused by ship motion can affect the ship power system. Considering these impacts are essential in power system stability and reliability analyses. (3) Manoeuvring conditions and the ship motion consequences on the power system have been unnoticed. Speed change and propulsion system torque fluctuations in manoeuvring conditions have significant effects on the power system. Inversely, power system fluctuations can cause a propulsion system speed change. This can affect the ship motion and should be considered in AES operation conditions. (4) The difference between the case study microgrids of the mentioned researches and a common terrestrial microgrid is often restricted to the load profile. It may not be similar to a ship microgrid in reality. The main difference between terrestrial microgrids and an AES power system is the unique dynamics of the propulsion system of the AES in different operational conditions. An integrated and compact model for an AES needs to focus on the unique dynamics of the propulsion system and consider the hydrodynamics of the marine vessel, too. In addition, it should provide the ability to analyse different operating conditions.

As the ship motion and associated mechanical concepts are essential for stability, control, and reliability studies of maritime power systems in varying conditions, an integrated model that includes both aspects is crucial. This paper proposes a comprehensive theoretical strategy for considering the linked effects of ship motion on the power system and vice versa. By deploying the proposed model-based approach, the ship power system analysis is not limited to predetermined load profiles inferred from specific operating conditions. In addition, the proposed method can accurately estimate the speed variation during route change manoeuvres. Although these fluctuations have substantial impacts on the high-speed vessels operation, it is not addressed adequately in the previous works. Moreover, the resistance forces' variations in a manoeuver are taken into account in the proposed approach. Concerning the ship variation in the track change operation, the speed control of the propellers is adjusted to keep the velocity within a specific range. Furthermore, the modified speed control approaches' impacts on the power system are analysed by employing the proposed model.

The rest of the paper is organized as follows. In Section 2, the framework of the proposed model for an AES and a typical power system model is presented. More information on the suggested model's hydrodynamics is given in Section 3. In Section 4, a mariner is studied according to the proposed model, and the advantages of the presented model are discussed. Finally, the main remarks of this work are concluded in Section 5.

2 | THE PROPOSED INTEGRATED MODEL FOR AN AES

The ship control system establishes a propeller speed reference to ensure that the ship maintains its desired speed or operational goals. The ship speed and its yaw angle behave according

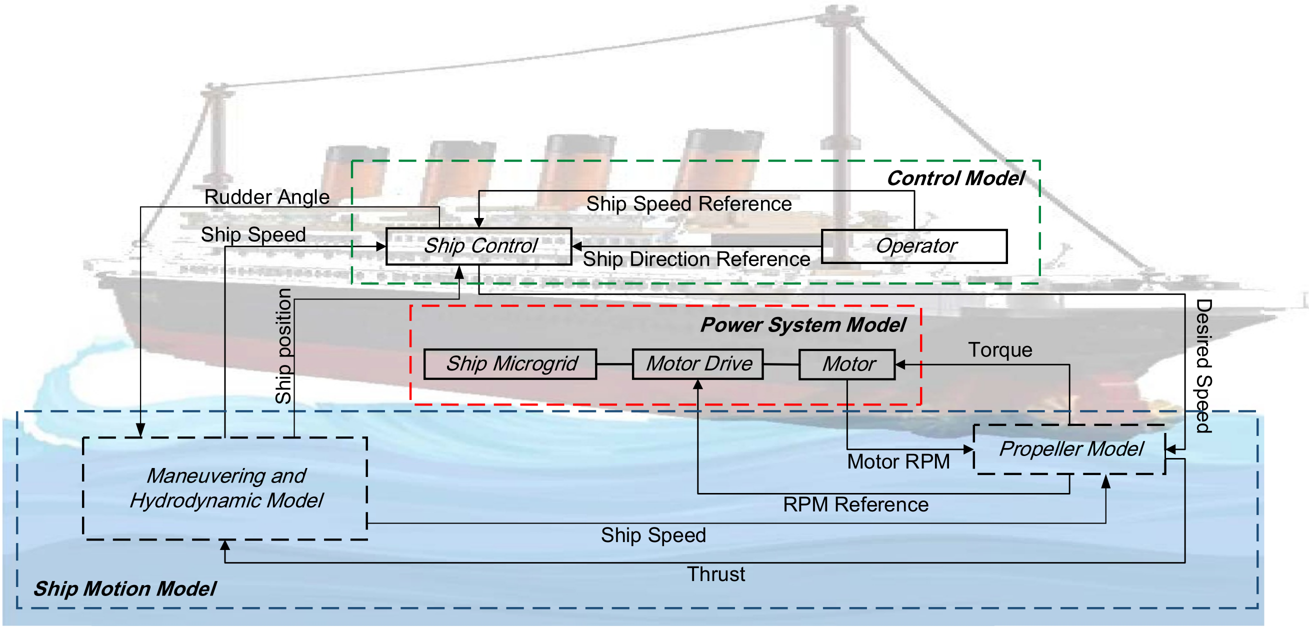

FIGURE 1 The proposed integrated model for the ship hydrodynamic and power system during a manoeuver operation

to hydrodynamic concepts and affect the propeller speed. Besides, the propeller thrust and torque are corresponded with its dynamic characteristics [19]. In the proposed model, these connections are thoroughly considered. Based on the mentioned relations, a framework for the proposed model is shown in Figure 1. It includes three main sections: (1) power system, (2) ship dynamic, and (3) control system. In the control section, the ship speed reference and route direction are defined. Also, the ship position, velocity, and related angles are monitored by various sensors [19, 20]. Details of the ship motion model are discussed in the next section.

According to Figure 1, once the operator commands a change in the ship speed, the propeller model calculates the desired speed for the propeller based on the ship desired speed. The RPM (round per minute) reference will be sent to the motor field-oriented control drive. Hence, the motor drive, which controls the propeller motor armature current, forces the shaft speed to reach the required speed. In addition, the propeller model calculates the produced thrust and yields the result to the manoeuvring and hydrodynamic model of the ship. On the other hand, the control system can change the direction of the ship route by changing the rudder angle [21, 22]. In the manoeuvring and hydrodynamic model, the position and speed change of the ship in a manoeuvring operation is obtained based on the ship velocity, the propeller thrust, and rudder angle.

A ship power system schematic diagram is demonstrated in Figure 2 [22, 23]. The propulsion motor is the primary load in a ship power system, and the unique dynamics of this load is the main focus of this paper. Thus, other loads have been grouped into hotel loads (like lighting, ventilation, and heating) and base loads. The power system voltage is considered to be 4.16 kV/60 Hz. Two types of electric power generators commonly manage the main loads in ships: (1) gas turbines and

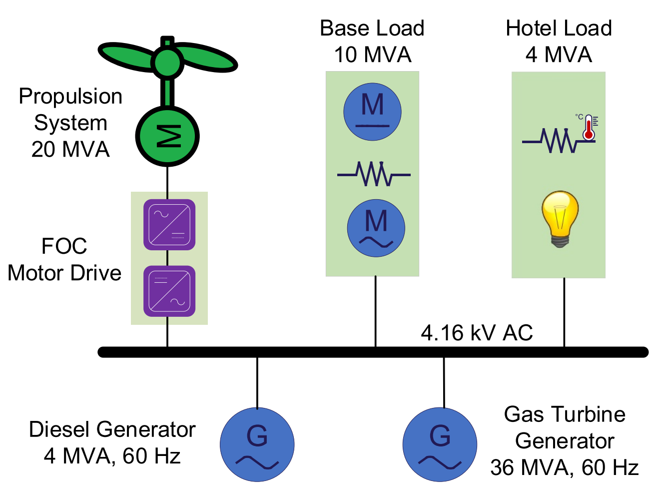

FIGURE 2 A notional ship power system

(2) diesel generators. The diesel generator has a lower fuel cost and starting time [24, 25]. The latter feature can increase the system stability and reliability in some operating scenarios. For instance, while a pumping motor is starting and the power system consumption exceeds the power generation for a limited time, the diesel generators can help the power system in shorter times. Although operating costs of gas turbines are elevated, high power density applications and low emission and space criteria necessitate their use in ships. The substantial benefit and merit can compensate for the additional expenses that gas turbine propulsion provides [26]. Thus, proper coordination and power-sharing between the types of generators based on the dominant operating condition can lead to substantial fuel savings and make ships greener and safer [27].

The selected power system for this study has a 36 MVA, round rotor gas turbine generator, and a 4 MVA, salient pole diesel generator. A field-controlled generator excitation system with uncontrolled rectifiers (AC1A type) controls the field voltages of the generators [28, 29]. Finally, a 20 MVA asynchronous motor is considered for the propulsion system. It is driven by a 12-pulse rotor field-oriented control motor drive. This type of motor drive orients the stator current with respect to the rotor flux in order to achieve an orthogonal spatial angle between the field flux and the armature magnetomotive force. As a result, the flux and torque can be separately adjusted [30].

3 | THE HYDRODYNAMICS AND SHIP MOTION

Different aspects of ship motion and hydrodynamics should be studied for more precise modelling of the ship propulsion system and its power oscillations. The ship dynamic model in Figure 1 consists of (1) the propeller model and (2) the hydrodynamic and manoeuvring model. Each of these two parts focuses on a specific aspect of the ship motion. Their details are presented in the following subsections.

3.1 | The open-water propeller characteristics

A propeller performance is often represented by two non-dimensional variables [31]: (1) Thrust coefficient (K_T) and (2) Torque coefficient (K_Q). These two indices are dependent on the geometrical characteristics of the propeller. The propeller thrust and torque can be expressed as follows.

$$T = K_T \rho n^2 D^4 \tag{1}$$

$$Q = K_Q \rho n^2 D^5 \tag{2}$$

where T is the propeller thrust, Q is the propeller torque, D is the propeller diameter, ρ is the water density, n is the rotational speed. Besides, these coefficients are associated with other hydrodynamic aspects [32], given as:

$$K_T = f_k\left(R_n, J_A, \frac{P}{D}, \frac{A_E}{A_o}, z, \frac{t_b}{c}\right) \tag{3}$$

$$K_Q = f_Q\left(R_n, J_A, \frac{P}{D}, \frac{A_E}{A_o}, z, \frac{t_b}{c}\right) \tag{4}$$

where P/D is the pitch diameter ratio, A_E/A_o is the blade area, and z is the number of propeller blades. Moreover, R_n is the Reynolds number and can be obtained using Equation (5) [32–34].

$$R_n = \frac{\rho n D^2}{\mu} \tag{5}$$

In Equation (5), μ is the viscosity of the fluid, which is water in this study. The Reynolds number aids in predicting the flow patterns in various fluid flow conditions [35]. The Lerb techniques can be used to account for the Reynolds number impact on propeller characteristics [32, 36]. Furthermore, in Equations (3) and (4), t_b/c is the maximum blade thickness ratio to the cord length at a characteristic radius. The advance coefficient, J_A, is obtained according to the velocity of advance, V_a, using Equation (6).

$$J_A = \frac{V_a}{nD} \tag{6}$$

V_a is the water flow speed through the propeller disc. Typically, this is the speed of the ship, but for a ship that has its propellers behind the hull, it could be reduced. For calculating J_A, it is necessary to calculate the velocity of advance. For a straightforward simulation, it is considered to be about equal to the ship velocity. However, the wake fraction should be taken into account for more precise modelling, as the ship hull shape causes uneven water flow velocity distribution behind it. It can result in a deviation of the advance velocity from the ship speed.

One common principle for considering the wake fraction in the ship motion model is the Taylor method. For axial velocities, the wake fraction can be expressed as Equation (7), in which $w_k$is wake fraction and U is the ship speed [31, 37].

$$w_T = 1 - \left(\frac{V_a}{U}\right) \tag{7}$$

Axial wake at a specific point in the propeller can be expressed as follows [38, 39]:

$$w_x(r) = \sum_{n=0}^{N} [a_n(r)\cos n\phi + b_n(r)\sin n\phi] \tag{8}$$

where a_n and b_n are the amplitudes of the Fourier components, r is the radius of the propeller, and φ is the angular position of a single blade. A wide variety of data on wake distributions, measured on a diversity of ships, is presented in Ref. [40]. Table 1 shows the extracted wake fraction model and the corresponding a_n and b_n for this study. For simplicity and without losing the model generality, we assume the axial wake is symmetric concerning vertical across the propeller axis.

TABLE 1 Fourier coefficients in wake fraction modelling

Symbol	Value
a0	0.05
$a1$	0.3
$a2$	3.75
$a3$	0.007

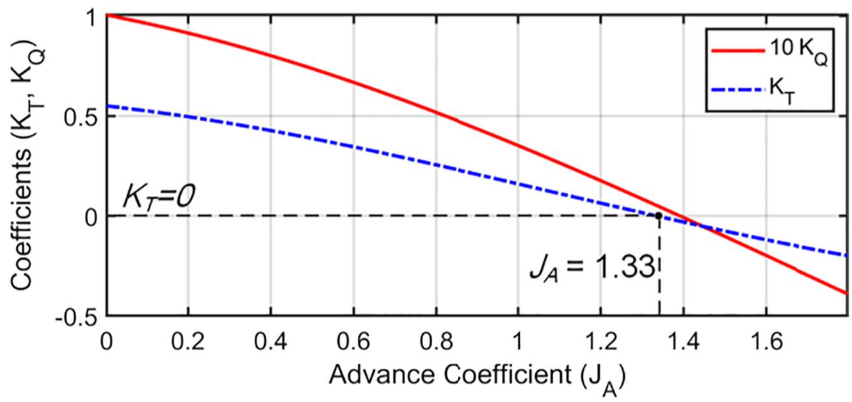

FIGURE 3 The thrust and torque coefficients with respect to advance coefficient for Wageningen B-series propeller

Thus, the decomposition only includes cosine terms, as seen in Table 1 [31, 38, 41].

Considering Equations (3) and (4), Equations (1) and (2) can be rewritten as follows:

$$T = f_k\left(R_n, J_A, \frac{P}{D}, \frac{A_E}{A_o}, z\right)\rho n^2 D^4 \tag{9}$$

$$Q = f_Q\left(R_n, J_A, \frac{P}{D}, \frac{A_E}{A_o}, z\right)\rho n^2 D^5 \tag{10}$$

The open-water characteristic of the Wageningen B-series propeller is extracted from [32], and thrust and torque coefficients concerning J_A are obtained after multiple regression analyses. K_T and K_Q curves are depicted in Figure 3. Table 2 shows the propeller parameters used in Figure 3. As shown in Figure 3, K_T is equal to zero at some point (here when J_A is 1.33). The propeller performs adjacent to this point when the ship attains its desired speed, and the ship acceleration will become restricted. However, there is a deviation in K_T from zero for managing with the resistance forces. The resistance forces and the resulted ship acceleration are addressed in the following subsection.

3.2 | The produced thrust model

The calculated propeller thrust and torque are employed in the ship motion analysis. The speed change caused by the produced thrust is obtained using Equation (11) [42].

$$m\dot{U} = T(1 - t_d) + R(U) \tag{11}$$

where m is the ship total mass, which includes the ship mass and the hydrodynamic added mass, and U is the ship velocity. For the propeller open-water hydrodynamic properties to be adjusted against the hull's neighbourhood, t_d, which is thrust deduction and a hull-propeller interaction factor, is employed [31]. In this study, t_d is considered equal to 0.2 [39]. $R(u)$ is the total resistance when the ship is voyaging forward. Resistance forces usually considered in $R(u)$ are frictional, wave-making, and wind [20]. In this study, R_F and R_R, which stand for the

TABLE 2 The ship and the propeller characteristics

Parameters	Value
P/D	1.25
A_E/A_o	0.65
Z	4
D	5.6 m
P	997 kg/m^3

frictional and the wake-making resistance, are derived from Equations (12) and (13) [31]:

$$R_F = C_f U^i A \tag{12}$$

$$R_R = C_R \rho U^2 A \tag{13}$$

where i depends on the shape of the ship. For standard ship surfaces, it is 1.825. C_f and C_R are the coefficients for the friction and the wave-making resistance, and A is the wetted area of the ship. Furthermore, wind forces in the surge and sway direction of the vessel are estimated using the following expressions for accounting for the effect of changing wind angle during a ship route change manoeuver.

$$F_{wind-X} = C_{airX}(\psi)\rho u^2 S \tag{14}$$

$$F_{wind-Y} = C_{airY}(\psi)\rho v^2 S \tag{15}$$

where C_{airX} and C_{airY} are coefficients of the wind force in the surge and sway direction, S is the facing area of the ship in the air, ψ is the wind direction, and u and v are the surge and sway velocities. C_f and C_R are attained following the approaches provided by [43]. The zero degrees of wind direction signifies that the wind is coming from the following direction, while the 180 degrees of wind direction indicates that the wind is a head wind. Figure 4 depicts the coefficients derived for each angle of wind direction and the wind speed of 10 m/s.

Another component added to the model for more precise results is the loss of effective disc area caused by the in-and-out-water effect. In extreme conditions, wave disturbances

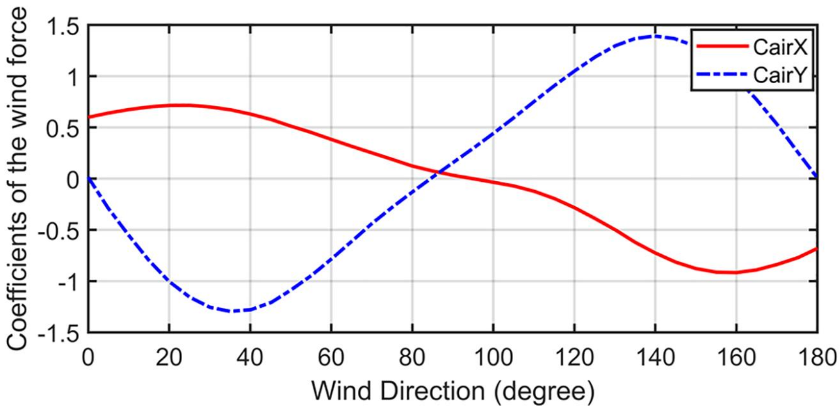

FIGURE 4 The wind force coefficients with respect to the wind direction for obtaining the wind resistance

can make parts of the propeller get out of the water. This will result in loss of thrust and shall be considered in the model in these conditions. This loss of effective thrust can be formulated in different forms. In Ref. [44], a simplified form for the loss of effect coefficient is proposed and is used in the proposed model.

$$\beta = 0.5 + 0.5(Min(1, Max(-1, h/R))) \tag{16}$$

where β denotes the loss factor for the in-and-out-water effect, h is the propeller shaft submergence, and R is the radius of the propeller. As can be deduced from Equation (16), when the propeller is entirely in water, h/R is more than 1, and the loss factor equals 1. Thus, the efficiency loss of thrust is equal to zero. Then, Equation (9) can be modified and rewritten as:

$$T = \beta f_k\left(R_n, J_A, \frac{P}{D}, \frac{A_E}{A_o}, z\right)\rho n^2 D^4 \tag{17}$$

3.3 | The manoeuvring model

Ship motion, stability, and control studies are traditionally separated into two main areas: sea-keeping and manoeuvring [19, 20]. The main purpose of the sea-keeping is the ship performance encountering waves and other resistances while keeping the same direction at a constant speed. In this regard, the study of steering characteristics of ships with forwarding speed and its response to the command of propulsion systems and control surfaces lies in the manoeuvring field of study. An important aspect that is not addressed in the literature of AES power systems is the kinetic model for manoeuvring operation of marine vessels. Thus, the state-of-the-art research methods for better functionality of ship power systems are not analysed in the manoeuvring conditions. This aspect becomes important when the ship control goal is to hold its speed at a specific range; as in manoeuvring conditions, the ship speed has unique fluctuations.

There are two approaches for the mathematical modelling of forces in manoeuvring. The first approach, commonly used in classical manoeuvring theory, is by utilizing the Taylor series. A truncated Taylor series with only odd terms of third order is presented [45]. The second approach is to use second order modulus terms [46]. In this paper, the first approach, which is more common in studies, is used. By applying concepts from [20, 45], forces in each direction can be acquired using Equations (18)–(20).

$$\begin{aligned} X = {} & X_u u + X_{uu}u^2 + X_{uuu}u^3 + X_{vv}v^2 + X_{rr}r^2 + X_{rv}rv \\ & + X_{\delta\delta}\delta^2 + X_{u\delta\delta}u\delta^2 + X_{v\delta}v\delta + X_{uv\delta}uv\delta \end{aligned} \tag{18}$$

$$\begin{aligned} Y = {} & Y_v v + Y_r r + Y_{vvv}v^3 + Y_{vvr}v^2 r + Y_{vu}vu + Y_{ru}ru \\ & + Y_\delta \delta + Y_{\delta\delta\delta}\delta^3 + Y_{u\delta}u\delta + Y_{uu\delta}u^2\delta + Y_{v\delta\delta}v\delta^2 \\ & + Y_{vv\delta v}v^2\delta + Y_0 + Y_{0u}u + Y_{0uu}u^2 \end{aligned} \tag{19}$$

$$\begin{aligned} Z = {} & Z_v v + Z_r r + Z_{vvv}v^3 + Z_{vvr}v^2 r + Z_{vu}vu + Z_{ru}ru \\ & + Z_\delta \delta + Z_{\delta\delta\delta}\delta^3 + Z_{u\delta}u\delta + Z_{uu\delta}u^2\delta + Z_{v\delta\delta}v\delta^2 \\ & + Z_{vv\delta}v^2\delta + Z_0 + Z_{0u}u + Z_{0uu}u^2 \end{aligned} \tag{20}$$

X and Y are the forces in the x and y directions, and Z is the moment around the z-axis. Y_0 and Z_0 are Y and Z in the initial equilibrium condition. u, v, and r are surge, sway, and yaw velocities, respectively. Finally, δ is the rudder angle. The coefficients in Equations (18)–(20) are called hydrodynamic derivatives. They are partial derivatives of X, Y, or Z with respect to motion parameters. The subscript notations denote these coefficients in the form of A_b, A_{bc}, and A_{bcd}, which are defined as follows:

$$A_b = \frac{\partial A}{\partial b} \tag{21}$$

$$A_{bc} = \frac{\partial^2 A}{\partial b\, \partial c} \tag{22}$$

$$A_{bcd} = \frac{\partial^3 A}{\partial b\, \partial c\, \partial d} \tag{23}$$

where ∂ is the partial derivative operator. A can be X, Y, or Z, and b, c, and d can be replaced by r, u, v, or δ. It should be noticed that some terms have been neglected considering the ship physical properties. These coefficients have been extracted by curve fitting and data analysis of the test results in Ref. [47]. After calculating forces and moments, state equations are obtained as:

$$\dot{u} = \frac{1}{\mathrm{m} - \mathrm{X}_{\dot{u}}} X\left(\frac{U^2}{L}\right) \tag{24}$$

$$\dot{v} = -\frac{\left(\left(-\mathrm{I}_z + \mathrm{Z}_{\dot{r}}\right)Y + \left(\mathrm{mX}_G - \mathrm{Y}_{\dot{r}}\right)Z\right)\left(\frac{U^2}{L}\right)}{\left(\mathrm{I}_z - \mathrm{Z}_{\dot{r}}\right)\left(\mathrm{m} - \mathrm{Y}_{\dot{v}}\right) - \left(\mathrm{mX}_G - \mathrm{Y}_{\dot{r}}\right)\left(\mathrm{mX}_G - \mathrm{Z}_{\dot{v}}\right)} \tag{25}$$

$$\dot{r} = \frac{\left(-\left(\mathrm{mX}_G - \mathrm{Z}_{\dot{v}}\right)Y + \left(\mathrm{m} - \mathrm{Y}_{\dot{v}}\right)Z\right)\left(\frac{U^2}{L^2}\right)}{\left(\mathrm{I}_z - \mathrm{Z}_{\dot{r}}\right)\left(\mathrm{m} - \mathrm{Y}_{\dot{v}}\right) - \left(\mathrm{mX}_G - \mathrm{Y}_{\dot{r}}\right)\left(\mathrm{mX}_G - \mathrm{Z}_{\dot{v}}\right)} \tag{26}$$

where m and I_z are mass and inertia of the ship, X_G is the distance of the centre of coordinates from the centre of ship gravity, L is the length of the vessel. $\dot{u}$, $\dot{v}$ and $\dot{r}$are accelerations according to X, Y, and Z directions. Thereby, the speed of the ship in manoeuvring can be obtained using the Euler equation as given in Equations (27)–(29). The instantaneous speed can be calculated by Equation (30) in the control system of the ship. Δt is the sample time of speed estimation used in the ship control system. and k and $k+1$ are indices that show the input and output of a variable in each iteration of the speed estimation, respectively.

$$v_{k+1} = v_k + \dot{v}\Delta t \tag{27}$$

$$u_{k+1} = u_k + \dot{u}\Delta t \tag{28}$$

$$r_{k+1} = r_k + \dot{r}\Delta t \tag{29}$$

$$U = \sqrt{v^2 + \left(U_0 + u\right)^2} \tag{30}$$

It should be noted that the hydrodynamics equations are based on the nominal speed of the ship. Thus, for considering the effect of the propeller thrust, the nominal speed should be changed according to the propeller dynamics. For this purpose, an algorithm for speed estimation in manoeuvring conditions is proposed, shown in Figure 5. This algorithm is based on the model framework in Figure 1. It shows that at every step of position estimation in the ship control system, the propeller motor speed and ship speed should be monitored, and their fluctuations should be considered in the manoeuvring equations. The advantages of the proposed algorithm are explored by simulating assumed manoeuvring scenarios in the next section.

4 | THE SIMULATION RESULTS

A mariner vessel is investigated in the MATLAB/Simulink simulation tool concerning the proposed model framework shown in Figure 1 and its related concepts. The studied ship has 48 kilotons of total mass and is 160 m in length. Also, its nominal speed is 7.71 m/s (15 knots) [47]. According to the power system model components, the step time of the simulation is adjusted to 60 μs. Two scenarios are defined and performed on the proposed model. In the first scenario, a manoeuvring operation condition is investigated utilizing the proposed model. This scenario illustrates and discusses the effects and necessity of interconnecting the electrical and hydrodynamic concepts for ship motion analysis. In the second scenario, one of the standard operations of a vessel [23] is analysed. Ship acceleration, a common operating goal in a vessel journey, is examined by the proposed model, and power system variations during this condition are investigated.

4.1 | The manoeuvring scenario

In this scenario, the operator of the ship commands for a change of route direction. Considering experimental measurements of the hydrodynamic derivatives in Ref. [47] that are used in this paper, it is assumed that the yaw angle of the ship should be changed by 40°. The ship position during this scenario is depicted in Figure 6, where the start time of the manoeuvring (the change of direction) is 6 s. According to the aim of this study for estimating the ship motion and its impacts on the ship power system during a route change manoeuver, it is assumed the ship is cruising in calm water. Thus, without losing the generality, the in-and-out-water effect is disregarded. However, the wind direction changes during this operation condition and the consequences on the ship speed and power system are explored using the provided model. The impact of employing different modelling approaches on the ship speed behaviour during the mentioned manoeuver is explored in this scenario. The first speed estimation approach is obtained by considering the provided model by previous works. As previously stated, its primary focus is on manoeuvring and hydrodynamic concepts during a manoeuver. Marine engineers commonly use this model for estimating the ship speed during a change of route operation. Notably, the interconnection between the power system and the ship hydrodynamic is not taken into account. Thus, the corresponding power system fluctuations cannot be observed thoroughly using this conventional modelling approach.

The second approach for acquiring the ship speed during the defined manoeuver is by employing the proposed interconnected model. The vessel speed fluctuations according to these approaches are shown in Figure 7. As the simulations revealed, the ship speed patterns are different between the mentioned strategies. Thus, another method is included in this scenario for a more thorough investigation of the manoeuvring effects on the ship power system. Unlike the other techniques that kept the shaft speed constant during this operating condition [20, 48], the proposed method has a ship speed control that keeps the ship speed within a margin of the target speed by altering the propeller speed. This margin should be determined based on the ship operating condition

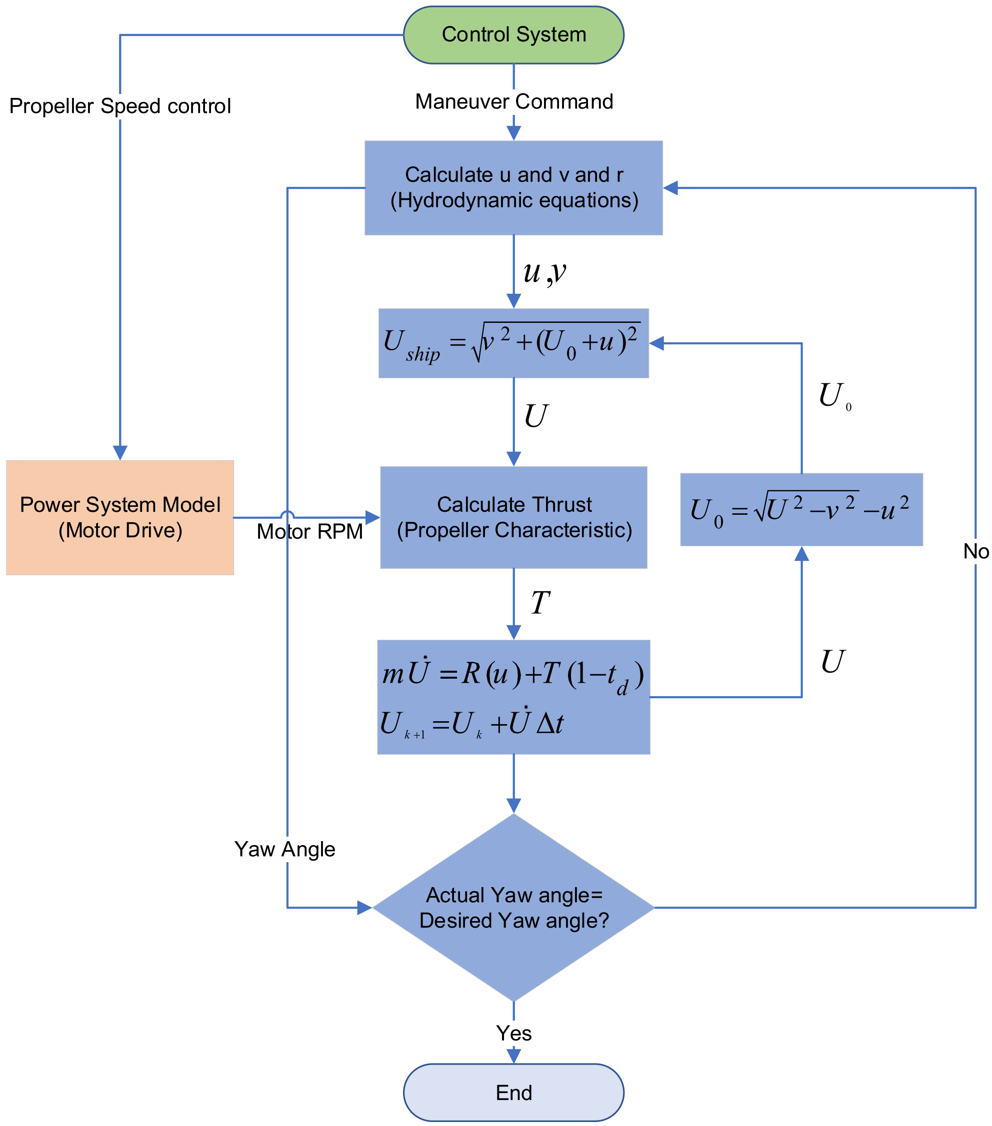

FIGURE 5 The proposed speed estimation algorithm for route change manoeuvring condition

[22]. For this study, the margin is considered to be 1% of the desired speed. Hence, when the ship speed exceeds the threshold, the motor drive receives a signal to change the propeller shaft speed to retain the speed in the specified range. In addition, the altering propeller speed is applied with a constant slope. As shown in Figure 7, the speed estimation deviation from the desired speed is about 1 knot without using the integrated model during the manoeuver. This variation is about 0.4 knots in the proposed model with the same conditions. The amplitude of the speed fluctuation is reduced to 0.2 knots by utilizing the improved propeller speed control. Therefore, the enhanced speed control system can reduce the ship speed variations by 50 percent. It is noteworthy that if the segregated approach is utilized for the speed estimation, the speed fluctuation reduction is 80 percent.

The source of this inequality in speed estimation is that while conventional models use ship motion concepts for this scenario, they assume U_0 in Equation (30) to be constant. They calculate u and v from Equations (27) and (28) by utilizing hydrodynamic Equations (18)–(26) and then the ship speed is obtained using Equation (30). Thus, U_0 is assumed to be 7.71 m/s for the first approach. However, this assumption is not realistic. In the steady-state, the ship speed remains constant. At this point, the propeller thrust should be equal to the resistance forces, and the ship acceleration should be around zero. When the speed of the ship decreases because of a manoeuver operation, J_A decreases according to Equation (6). Therefore, K_T increases and the propeller system produces more thrust. It means that in Equation (30) the propeller thrust and the resulting acceleration should be considered. For this reason, the propeller speed change and its effects on the ship speed are considered in the proposed algorithm. In summary, the remarkable difference between these approaches is because the proposed model correctly represents the hydrodynamic and electrical system interactions. Thus, the proposed method for restricting the ship speed during the manoeuver is more dependable. Since this difference is noticeable and can affect the ship's design level and control system decisions, it can be utilized to precisely design control systems in future works.

Furthermore, the power system fluctuations in the manoeuvring operation are analysed using the presented speed change strategies. In the proposed variable speed model, the ship controller keeps the speed of the ship in a specified range. For this goal, the speed reference of the motor shaft changes during the manoeuver in this approach. This variation results in torque changes in the propeller. Utilizing the proposed integrated model, the effect of this manoeuvring scenario on the ship power system is studied. The propeller torque, power system voltage, and electrical power consumption are depicted in Figures 8–10, respectively. In the constant speed approach, the torque and power fluctuations are smoother. But when the speed of the propeller becomes a control parameter for keeping the speed of the ship constant, the torque and power have more fluctuations. As the speed of the ship gets lower than the speed limit, the motor drive starts to change the speed of the propeller, and according to the ship motion relations, the torque of the propeller increases. When the speed of the ship gets back to the desired margin, the speed of the propeller decreases again, reducing the torque and power consumption of the propeller motor. As a penalty of keeping the speed ship in a restricted margin, the sudden changes of power and torque in the variable speed approach have resulted in voltage fluctuations in this approach. But the voltage fluctuation amplitude is not significant, shown in Figure 9. In addition, these fluctuations can cause wear and tear for the propeller shaft. Loss of lifetime in electrical components of the ship power system during different operating conditions will be studied in future works using the proposed integrated model.

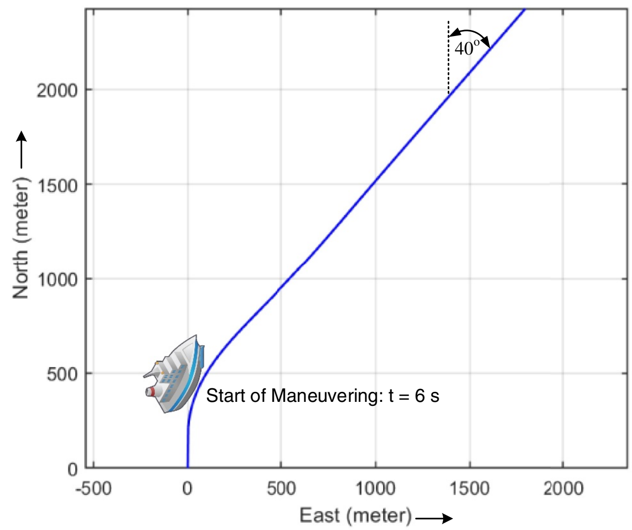

FIGURE 6 The ship position during the ship route change manoeuver scenario

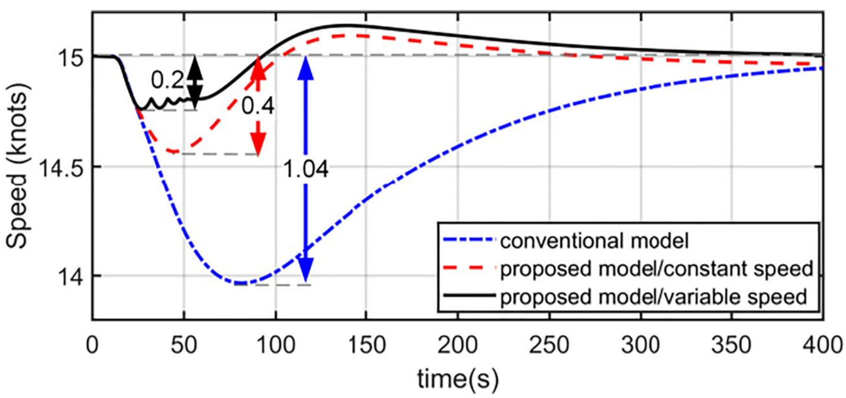

FIGURE 7 The ship speed estimation in the route change manoeuver using the segregated model and the proposed model with propeller speed (a) constant and (b) variable to keep the ship speed constant

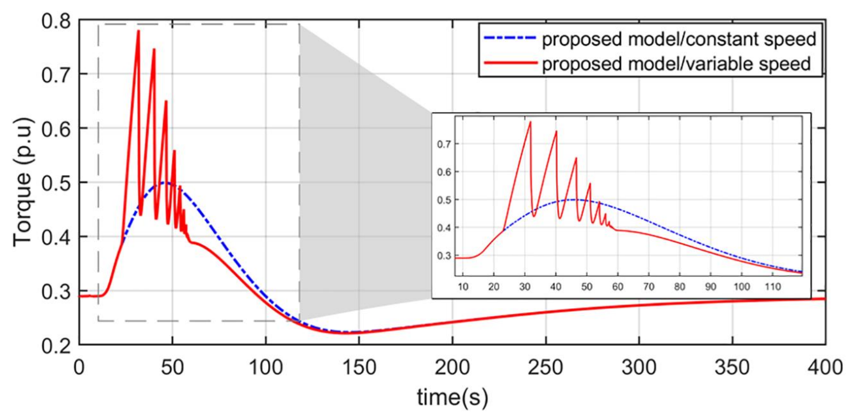

FIGURE 8 The propeller torque in the route change manoeuver using the proposed model with propeller speed (a) constant and (b) variable to keep the ship speed constant

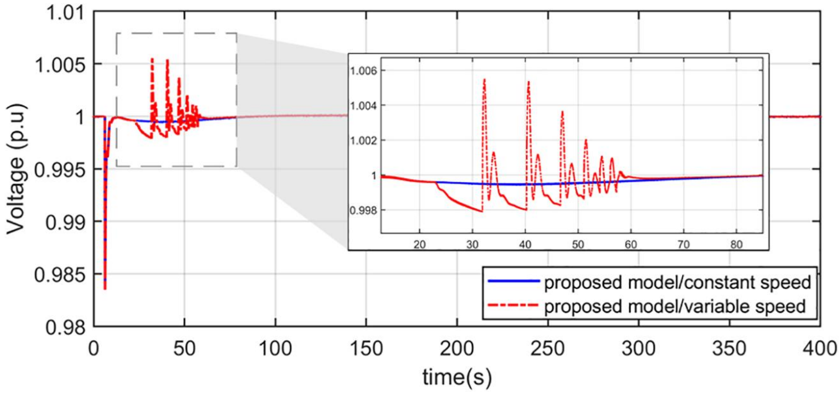

FIGURE 9 The power system voltage in the route change manoeuver using the proposed model with propeller speed (a) constant and (b) variable to keep the ship speed constant

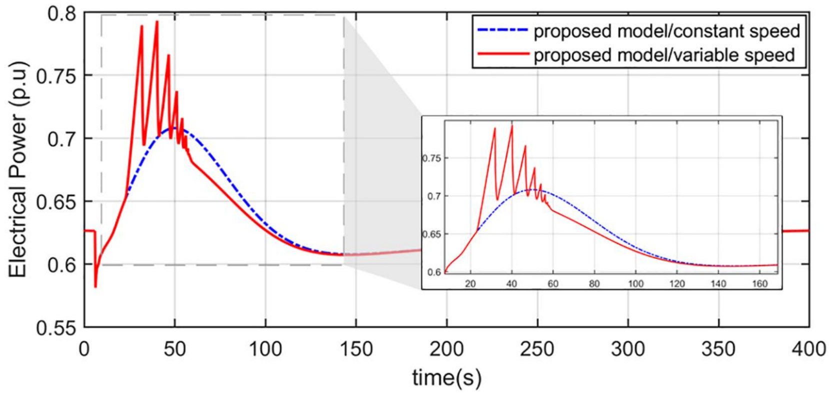

FIGURE 10 The propulsion power in the route change manoeuver using the proposed model with propeller speed (a) constant and (b) variable to keep the ship speed constant

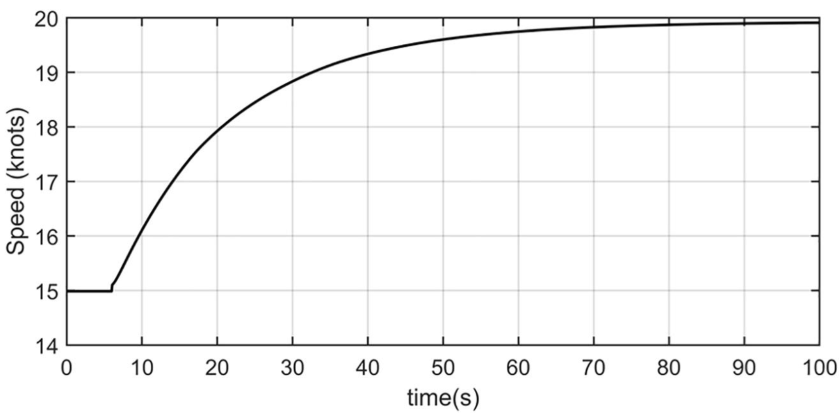

FIGURE 11 The ship speed variation in the speed increase manoeuver scenario employing the proposed integrated model

4.2 | The ship speed increase scenario

In this scenario, a typical ship operating scenario is studied. It is presumed that the operator raises the reference speed for the ship by 25 percent. For more accuracy, the ship resistances and the wake fraction are taken into account in this scenario. When the command of speed rise reaches the propulsion motor drive, it increases the speed of the rotor to its maximum possible level until the ship reaches the desired speed. After that, it specifies a speed for the motor in which the overall thrust of the ship becomes equal to the resistance forces. Thus, the ship speed remains steady. The rate of speed rise can be seen in Figure 11. In Figure 12, the propulsion system power fluctuations are shown. While the ship speed is increasing, the overall power consumption of the propulsion system rises.

After the ship reaches the desired speed, ship motion effects result in voltage and frequency fluctuations. These fluctuations are depicted in Figures 13 and 14, respectively. It can be seen that the voltage drops up to 6.2% during the ship acceleration. Also, at different speeds, the effects of ship resistance, waves, and wake fraction on the voltage of the power system are different. Thus, the voltage variations depend on the model's precision in the ship motion analysis. This also applies to frequency fluctuations. It can be deduced from Figure 14 that the frequency

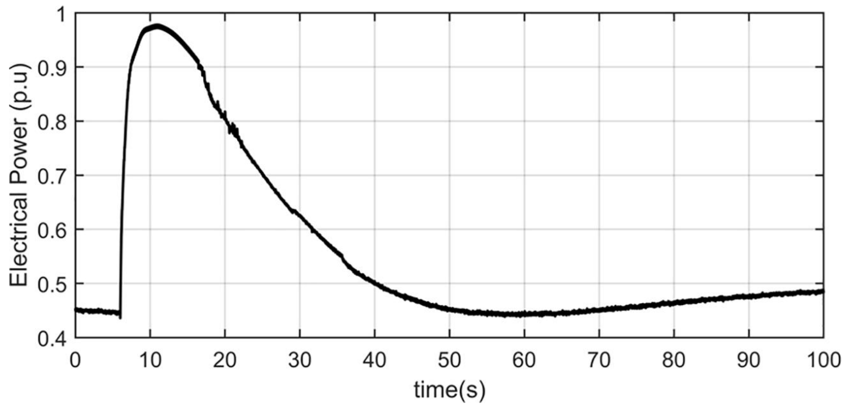

FIGURE 12 The power of propulsion system fluctuations during the speed increase manoeuver scenario using the proposed integrated model

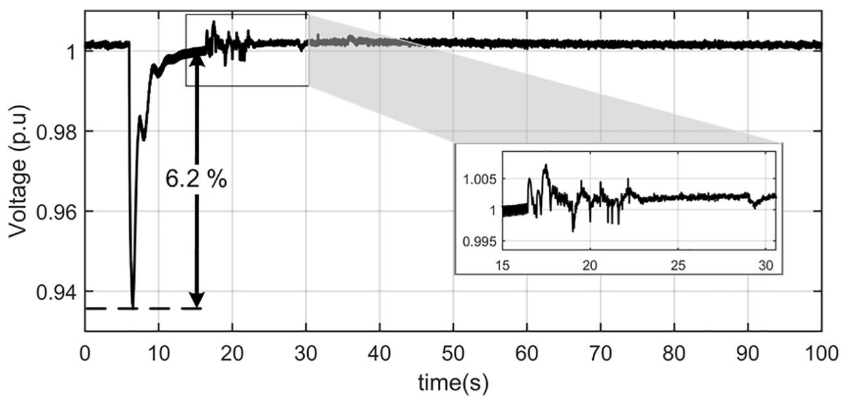

FIGURE 13 The power system voltage fluctuations during the speed increase manoeuver scenario using the proposed integrated model

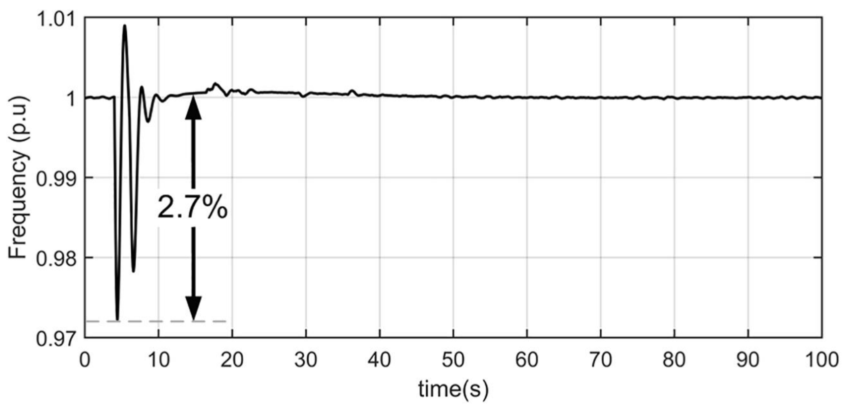

FIGURE 14 The power system frequency fluctuations during the speed increase manoeuver scenario using the proposed integrated model

fluctuations at the beginning of the speed change are up to 2.7%. Even after the ship reaches its final speed, the power system frequency has fluctuations because of the wake fraction and wave effects. These fluctuations are essential in the power quality analysis of the ship power system and can be extracted in different operational conditions using the proposed model. As mentioned, in the conventional methods, the interactions of hydrodynamic and electrical power systems are not considered comprehensively. Thus, the simulation results of this scenario using the proposed theoretical model cannot be compared with the conventional models.

5 | CONCLUSION

In this paper, an integrated theoretical model to address the impacts of AES motion on its power system and vice versa during a manoeuvring operation is proposed. For this target, the ship hydrodynamic, propeller dynamic, and power system models of a typical marine vessel are explored in detail. In addition, considering this model, a comprehensive algorithm for estimating the ship speed thoroughly during a direction change manoeuvring is proposed. Then, the efficacy of deploying the presented model in evaluating ship state is investigated using simulation methods. It is revealed that the suggested model outperforms the current unintegrated models by 60% in terms of speed fluctuation amplitude estimation. Thus, this distinction, as well as the benefits of the proposed approach, are discussed. The propeller speed control is then enhanced to keep the ship speed within a narrow range, which is vital in specific operating situations. The modified speed control reduces ship speed fluctuations by 80% compared to conventional approaches and 50% compared to the accurate suggested model. Furthermore, the proposed model capacity in evaluating the impacts of ship motion on power system fluctuations is assessed through a ship acceleration scenario. It is demonstrated that this model can investigate the mutual effects of ship motion and power system precisely in this scenario.

Since the proposed model and the speed estimation approach considers different aspects of the ship manoeuvring circumstances, it can be utilized to improve the AESs power management system from an interdisciplinary perspective. As a result of adequately analysing diverse conditions, the power management system design will efficiently perform both electrically and mechanically. In future works, this theoretical model will be validated using experimental methods. Also, it will be deployed to enhance the electric power management systems to reduce propellers' mechanical fatigue and increase their lifespan during a manoeuver situation.

NOMENCLATURE

Indices and sets

k	Index for the number of the speed estimation sample

Parameters and constants

A	Wetted area of the ship
A_E/A_o	Propeller blade area
c	Length of the blade cord
C_f	Frictional resistance coefficient of the ship
C_{airX}	Coefficients of the wind force in surge direction
C_{airY}	Coefficients of the wind force sway direction
D	Diameter of the propeller
I_z	Inertia of the ship
K_T	Thrust coefficient for the open-water characteristic of the propeller
K_Q	Torque coefficient for the open-water characteristic of the propeller
L	Length of the ship
m	Total mass of the ship
n	Rotational speed of the propeller
P	Pitch of the propeller
Q	Torque of the propeller
r	Radius of the propeller
R_n	The Reynold's number
S	Facing area of the ship in the air
ψ	The wind direction
T	Thrust of the propeller
t_b	Blade thickness
t_d	Thrust deduction factor
Δt	sample time of speed estimation
z	Number of propeller blades
ρ	Density of water
μ	Viscosity of water

Variables

β	The in-and-out-water effect loss factor
a_n, b_n	Fourier components amplitudes of wake fraction
$F_{wind\text{-}X}$	Wind force in surge direction
$F_{wind\text{-}Y}$	Wind force in sway direction
h	Propeller immersion depth
J_A	The advance coefficient
$R(u)$	Total resistance of the ship
R_F	Frictional resistance of the ship
R_R	Wake-making resistance of the ship
U	Ship velocity
u, v, r	Surge, sway, and yaw velocities of ship
V_a	The velocity of advance
w_k	Wake fraction for axial velocities
X, Y	Applying forces to the ship in x, y direction
X_G	Coordinates centre distance from the gravity centre of the shop
Y_0, Z_0	Y, Z in initial equilibrium condition
Z	Ship moment around z-axis
φ	Angular position of a single propeller blade
δ	Rudder angle

DATA AVAILABILITY STATEMENT

Data sharing not applicable to this article as no datasets were generated or analyzed during the current study.

ORCID

Saman Nasiri https://orcid.org/0000-0002-8072-7714
Saeed Peyghami https://orcid.org/0000-0003-0670-3375

REFERENCES

1. Ouroua, A., Domaschk, L., Beno, J.H.: Electric ship power system integration analyses through modeling and simulation. In: 2005 IEEE Electric Ship Technologies Symposium, pp. 70–74 (2005)
2. Seenumani, G., Sun, J., Peng, H.: Real-time power management of integrated power systems in all electric ships leveraging multi time scale property. IEEE Trans. Control Syst. Technol. 20(1), 232–240 (2012)
3. Kanellos, F.D., Tsekouras, G.J., Prousalidis, J.: Onboard DC grid employing smart grid technology: challenges, state of the art and future prospects. IET Electr. Syst. Transp. 5(1), 1–11 (2015)
4. Hou, J., Sun, J., Hofmann, H.: Adaptive model predictive control with propulsion load estimation and prediction for all-electric ship energy management. Energy. 150, 877–889 (2018)
5. Zhang, J., et al.: Restraining integrated electric propulsion system power fluctuation using hybrid energy storage system. In: 2015 IEEE International Conference on Mechatronics and Automation (ICMA), pp. 336–340 (2015)
6. Tsekouras, G.J., Kanellos, F.D., Prousalidis, J.: Simplified method for the assessment of ship electric power systems operation cost reduction from energy storage and renewable energy sources integration. IET Electr. Syst. Transp. 5(2), 61–69 (2015)
7. Skjong, E., et al.: System-wide harmonic mitigation in a diesel-electric ship by model predictive control. IEEE Trans. Ind. Electron. 63(7), 4008–4019 (2016)

8. Radan, D., et al.: Reducing power load fluctuations on ships using power redistribution control. Mar. Technol. SNAME News. 45(3), 162–174 (2008)
9. Kanellos, F.D.D., et al.: An effort to formulate frequency modulation constraints in ship-electrical systems with pulsed loads. IET Electr. Syst. Transp. 1(1), 18–28 (2011)
10. Kanellos, F.D., et al.: Effort to formulate voltage modulation constraints in ship-electrical systems with pulsed loads. IET Electr. Syst. Transp. 2(1), 18–28 (2012)
11. Park, D., Zadeh, M.K.: Dynamic modeling and stability analysis of on-board DC power system for hybrid electric ships. In: 2019 IEEE Transportation Electrification Conference and Expo (ITEC), pp. 1–6 (2019)
12. Haseltalab, A., Botto, M.A., Negenborn, R.R.: Model predictive DC voltage control for all-electric ships. Control Eng. Pract. 90, 133–147 (2019)
13. Arcidiacono, V., Monti, A., Sulligoi, G.: Generation control system for improving design and stability of medium-voltage DC power systems on Ships. IET Electr. Syst. Transp. 2(3), 158–167 (2012)
14. Apsley, J.M., et al.: Propulsion drive models for full electric marine propulsion systems. IEEE Trans. Ind. Appl. 45(2), 676–684 (2009)
15. Elders, I.M., et al.: Modelling and analysis of electro-mechanical interactions between prime-mover and load in a marine IFEP system. In: IEEE Electric Ship Technologies Symposium, ESTS 2007, pp. 77–84 (2007)
16. Nasiri, S., et al.: An open-water efficiency based speed change strategy with propeller lifespan enhancement in all-electric ships. IEEE Access. 9, 22595–22604 (2021)
17. Bø, T.I., et al.: Marine vessel and power plant system simulator. IEEE Access. 3, 2065–2079 (2015)
18. Zahedi, B., Norum, L.E.: Modeling and simulation of all-electric ships with low-voltage DC hybrid power systems. IEEE Trans. Power Electron. 28(10), 4525–4537 (2013)
19. Fossen, T.I.: Handbook of Marine Craft Hydrodynamics and Motion Control. John Wiley and Sons, Chichester (2014)
20. Perez, T.: Ship Motion Control; Course Keeping and Roll Stabilisation using Rudder and Fins. Springer, London (2005)
21. Fossen, T.I.: Guidance and Control of Ocean Vehicles. John Wiley and Sons, Chichester (1999)
22. Ådnanes, A.K.: Maritime Electrical Installations and Diesel Electric Propulsion. ABB Marine AS, Oslo (2003)
23. Kalsi, S.S., Nayak, O.: Ship electrical system simulation. In: IEEE Electric Ship Technologies Symposium, pp. 63–69 (2005)
24. Smil, V.: Prime Movers of Globalization: The History and Impact of Diesel Engines and Gas Turbines. MIT Press, Cambridge (2013)
25. Vicenzutti, A., Menis, R., Sulligoi, G.: All-electric ship-integrated power systems: dependable design based on fault tree analysis and dynamic modeling. IEEE Trans. Transp. Electrif. 5(3), 812–827 (2019)
26. Sanneman, B.N.: Pioneering gas turbine-electric system in cruise ships: a performance update. Mar. Technol. SNAME News. 41(4), 161–166 (2004)
27. Sorensen, A.J., et al.: Toward safer, smarter, and greener ships: using hybrid marine power plants. IEEE Electrif. Mag. 5(3), 68–73 (2017)
28. IEEE recommended practice for excitation system models for power system stability studies. Standard 421.5-2016, Revision of IEEE Std 421.5- 2005, IEEE (2016)
29. Kundur, P.S.: Power System Stability and Control, 1st ed. McGraw-Hill, New York (2009)
30. Bose, B.K.: Power Electronics and Variable Frequency Drives: Technology and Applications. Wiley, Hoboken (1996)
31. Carlton, J.: Marine Propellers and Propulsion, 4th ed. Butterworth-Heinemann, Oxford (2012)
32. Bernitsas, M., Ray, D., Kinley, P.: KT, KQ and Efficiency Curvers for Wageningen B-Series. Univ. Michigan, Ann Arbor (1981)
33. Nagamatsu, T.: A method for predicting ship wake from model wake. J. Soc. Nav. Archit. Jpn. 146, 43–52 (1979)
34. Phillips, A.B., Turnock, S.R., Furlong, M.: Evaluation of manoeuvring coefficients of a self-propelled ship using a blade element momentum propeller model coupled to a reynolds averaged navier stokes flow solver. Ocean Eng. 36(15–16), 1217–1225 (2009)
35. Ohashi, K.: Numerical study of roughness model effect including low-reynolds number model and wall function method at actual ship scale. J. Mar. Sci. Technol. 26(1), 24–36 (2021)
36. Van Oossanen, P., Oosterveld, M.W.C.: Further computer-analyzed data of the Wageningen B-Screw Series. Int. Shipbuild. Prog. 22, 251–262 (1975)
37. Saettone, S., et al.: Experimental measurements of propulsive factors in following and head waves. Appl. Ocean Res. 111, 102639 (2021)
38. Lewis, E.V.: Principles of Naval Architecture (Second Revision), Volume II - Resistance, Propulsion and Vibration - Relation of Hull Form to Resistance. The Society of Naval Architects and Marine Engineers (1988)
39. Hou, J.: Control and optimization of electric ship propulsion systems with hybrid energy storage. Ph.D. Thesis, Department of Mechanical Engineering, University of Michigan, USA (2017)
40. Cheng, H.M., Hadler, J.B.: Analysis of experimental wake data in way of propeller plane of single and twin screw ship. Trans. Soc. Nav. Arch. Mar. Eng. 73, 287–414 (1965)
41. Smogeli, N.: Control of marine propellers from normal to extreme conditions. Ph.D. Thesis, Department of Marine Technology, Norwegian University of Science and Technology (NTNU), Trondheim, Norway (2006)
42. Blanke, M., Pivano, L., Johansen, T.A.: An efficiency optimizing shaft speed control for ships in moderate seas," IFAC Proc. 7(1), 329–336 (2007)
43. Fujiwara, T., Ueno, M., Ikeda, Y.: Cruising performance of a large passenger ship in heavy sea. In: Proceedings of the International Offshore and Polar Engineering Conference, pp. 304–311 (2006)
44. Koushan, K.: Environmental and interaction effects on propulsion systems used in dynamic positioning, an overview. In: Proceedings of 9th International Symposium on Practical Design of Ships and other Floating Structures PRADS, pp. 1013–1020 (2004)
45. Abkowitz, B.M.A.: Ship hydrodynamics - steering and manoeuvrability. Hydro-and Aerodynamics Laboratory, Hydrodynamics Section, Lyngby, Denmark, Report No. Hy-5, Lectures (1964)
46. Fedayevsky, K.K., Sobolev, G.V.: Control and Stability in Ship Design. State Union Shipbuilding Publishing House, Leningrad (1963)
47. Chislett, M.S., Strom-Tejsen, J.: Planar motion mechanism tests and full-scale steering and manoeuvring predictions for a mariner class vessel. Int. Shipbuild. Prog. 12(129), 201–224 (2018)
48. Triantafyllou, M.S., Hover, F.S.: Maneuvering and control of marine vehicles, pp. 105–110. https://ocw.mit.edu/courses/mechanical-engineering/2-154-maneuvering-and-control-of-surface-and-underwater-vehicles-13-49-fall-2004/lecture-notes/1349_notes.pdf (2003)

How to cite this article: Nasiri, S., et al.: A comprehensive theoretical approach for analysing manoeuvring effects on ships by integrating hydrodynamics and power system. IET Electr. Syst. Transp. 12(2), 89–101 (2022). https://doi.org/10.1049/els2.12040